Journal of Applied Physics

RESEARCH ARTICLE | AUGUST 06 2012

Effective dielectric constant of two phase systems: Application to mixed conducting systems

Vladimir Petrovsky; Piotr Jasinski; Fatih Dogan

J. Appl. Phys. 112, 034107 (2012)
https://doi.org/10.1063/1.4743985

AIP Publishing

Effective dielectric constant of two phase systems: Application to mixed conducting systems

Vladimir Petrovsky,[1] Piotr Jasinski,[2] and Fatih Dogan[1]
[1]*Department of Materials Science and Engineering, Missouri University of Science and Technology, Rolla, Missouri 65409, USA*
[2]*Faculty of Electronics, Telecommunications and Informatics, Gdansk University of Technology, Gdansk 80-233, Poland*

(Received 21 September 2011; accepted 11 July 2012; published online 6 August 2012)

Theoretical approaches to electrical characterization of two phase systems are mostly limited to the systems where the individual components exhibit the same type of conductivity (pure dielectric or pure conductive systems). In this article, the brick wall geometry is extended to the mixed conductive systems with percolation. Impedance spectroscopy techniques were used for experimental investigation of slurries. Various metal oxide powders and host liquids were analyzed using a wide range of solids loadings. Comparison of experimental results with theoretical predictions shows good fitting of the experimental data. Parameters (the values of permittivity for both phases and percolation threshold) calculated from this fitting match the corresponding values of components of two phase systems. Analysis of both low frequency (less than 10 kHz) as well as high frequency (10 kHz to 1 MHz) responses of impedance spectra allows determining of permittivity of dielectric powders suspended in various liquids. Low frequency response provides better accuracy for systems with high dielectric contrast between components, while high frequency response is more accurate for low contrast systems. © *2012 American Institute of Physics*. [http://dx.doi.org/10.1063/1.4743985]

INTRODUCTION

Various theoretical models have been implemented towards electrical characterization of two phase systems. After initial introduction by Lorenz and Maxwell, the effective media approach undergone series of improvements in application to pure conductive and pure dielectric systems.[1–3] Several other approaches were also developed including the brick wall model.[1,4] Important directions of further advancements in the theoretical field include extension of theoretical models on the systems with mixed conductivity and introduction of percolation.[5–7] These extensions in the modeling and systematic experimental investigation of mixed conducting two phase systems with percolation can provide useful information for various practical applications.[8–11] Such investigations of two phase systems were performed earlier in our laboratory using suspensions of metal-oxide powders in organic solvents (slurries) by impedance spectroscopy techniques.[12–14] Measurements using slurries have some obvious advantages for a broader-range investigation in comparison with other types of two phase systems such as polymer-ceramic composites. It is relatively simple to control the electrical conductivity of solvents in slurries so that impedance spectroscopy techniques can be implemented more efficiently as a characterization method. The dielectric contrast between the liquid and suspended particles in slurries can be adjusted by using solvents with different values of permittivity. Effects of particle sedimentation and agglomeration on dielectric properties of slurries can be minimized by using efficient dispersion techniques such as ultrasonic processing. Our previous studies were focused on the low frequency part of the impedance spectra (less than 10 kHz) and extracting the values for the permittivity of powders. Conclusions of these studies include the following: (1) impedance spectra of slurries consist of two relaxation processes, (2) low frequency relaxation is caused by the permittivity of powder, and (3) permittivity of the liquid does not influence the low frequency part of the spectra. Values of permittivity for different materials in powder form could be determined by analyzing the low frequency part of impedance spectra of slurries. Another conclusion of these studies was that high frequency relaxation in impedance spectra is caused by permittivity of the liquid and not affected by the permittivity of powders in the slurry. These findings were confirmed by using small ceramic cubes submerged in the liquid as a physical model of slurries.[15]

The focus of the present article is on the high frequency part of the impedance spectra obtained from two phase systems with mixed conductivity. Procedures allowing a detailed material characterization are described by analyzing impedance spectra along with the theoretical equations. Validity of the theoretical approach is confirmed by analyzing of experimental (real) mixed conductive systems using impedance spectroscopy techniques.

PHASE DISTRIBUTION AND PERCOLATION

Effective media theory and brick wall methods are two fundamentally different approaches applied for two phase system modeling. Physical nature of effective media models (like Maxwell Wagner model) does not consider percolation, i.e., physical contacts between suspended particles irrespective of the suggested particle shape. The shape of particles influences effective permittivity of the mixture only through

dipole moments generated by particles. In these models, percolation parameters can be introduced only empirically (for example, by introducing partial clustering in the system[16]). The standard brick wall model describes a specific case of material distribution within a two phase system. Particles as the suspended phase are periodically distributed perfect cubes and they are disconnected in all ranges of particle volume fractions X_1 until the entire volume is filled ($X_1 = 1$) which describes two phase systems without percolation (percolation threshold $X_P = 1$). A detailed comparison of Maxwell Wagner and brick wall models was discussed in Ref. 15 using physical modeling as experimental approach.

Real systems always percolate earlier ($X_P < 1$) since the particle shape and distribution are different from that used in standard brick wall model. An additional parameter (or parameters) needs to be introduced in the model to address these differences. Various theoretical approaches were used to address this issue in Ref. 17. It was shown that main advantage of the brick wall approach is the possibility of natural extension on percolating systems. The brick wall model considers physical contacts between particles so that percolation can be introduced simply by changing the shape of suspended particles as shown in Fig. 1. A cube cell with a unit size of composite material is depicted as an element of the periodic brick-wall structure. The suspended component is shown as a dark cube inside the cell. It can be elongated in direction of electrical field ($\alpha > 1$) or suppressed ($\alpha < 1$) resulting in a columnar or layered type percolation, respectively. Volume fraction of the suspended material (X_1) is equal to $X_1 = \alpha x a^3$. Columnar type percolation will take place for $\alpha > 1$ when suspended particles will touch each other vertically at $\alpha x a = 1$. Substitution of $a = 1/\alpha$ in equation defining volume fraction of suspended material gives value of percolation threshold (X_P) which will be equal to the inverse square of percolation parameter ($X_P = 1/\alpha^2$). Layered type of percolation will dominate for $\alpha < 1$ when suspended particles are in contact horizontally at $a = 1$. Substitution of $a = 1$ in equation defining volume fraction of suspended material gives the value of percolation threshold (X_P) which, in this case, will be equal to percolation parameter ($X_P = \alpha$).

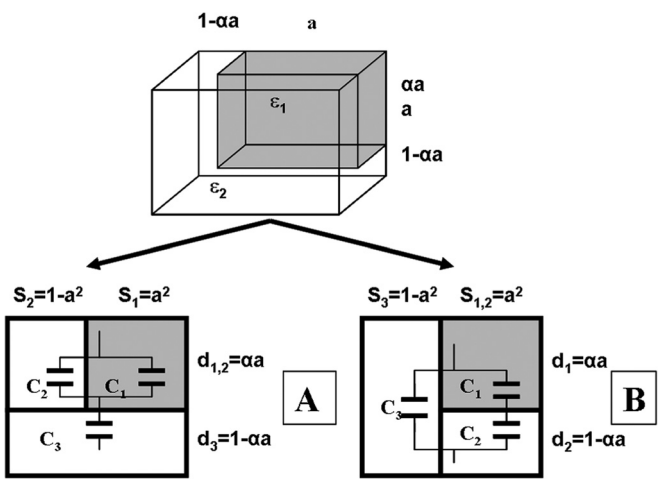

FIG. 1. Brick-wall model of two phase systems with elongated bricks causing percolation. Two possible transitions to equivalent circuit demonstrated: model 1 (a) and model 2 (b).

Additional advantage of brick wall model is natural transition from complex three dimensional distribution of electrical field to simple equivalent circuit which was described for cubic particles in Ref. 15 and extended on elongated particles in Ref. 17. It generates two models surrounding the exact solution as shown in Figs. 1(a) and 1(b). Corresponding equations as described in Ref. 17 are

$$\text{Model1}^*: \quad \frac{\varepsilon_{EFF}}{\varepsilon_2} = \frac{1}{1-(x_1\alpha^2)^{1/3} + \frac{(x_1\alpha^2)^{1/3}}{1-\left(\frac{x_1}{\alpha}\right)^{2/3}}\left(1-\frac{\varepsilon_1}{\varepsilon_2}\right)}, \tag{1}$$

$$\text{Model2}^*: \quad \frac{\varepsilon_{EFF}}{\varepsilon_2} = 1-\left(\frac{x_1}{\alpha}\right)^{2/3} + \frac{\left(\frac{x_1}{\alpha}\right)^{2/3}}{1-(x_1\alpha^2)^{1/3}\left(1-\frac{\varepsilon_2}{\varepsilon_1}\right)}. \tag{2}$$

It is reasonable to suggest that averaging of Eqs. (1) and (2) will provide good fitting for real two phase systems with percolation

$$\text{Averaging}: \quad \bar{\varepsilon}_{EFF} = \left(\varepsilon_{EFF}(\text{Mod.1})^*\varepsilon_{EFF}(\text{Mod.2})\right)^{1/2}. \tag{3}$$

As shown in Fig. 2, brick wall model modified with percolation parameter (Eqs. (1)–(3)) was compared with experimental results.[17,18] The experimental data were obtained from measurements using barium titanate (BTO) slurries (blue up triangles) and porous bulk samples of barium titanate prepared by sintering of powders with various amounts of fugitive pore providers, so that the data cover the entire range of barium titanate volume fractions X_1 from 0 to 1. A theoretical model (Eqs. (1)–(3)) was applied for nonlinear fitting using the software program in ORIGIN. This model presents $\varepsilon_{eff}(X_1)$ dependence with three parameters (ε_1, ε_2, and α) which were calculated by the software program as a result of

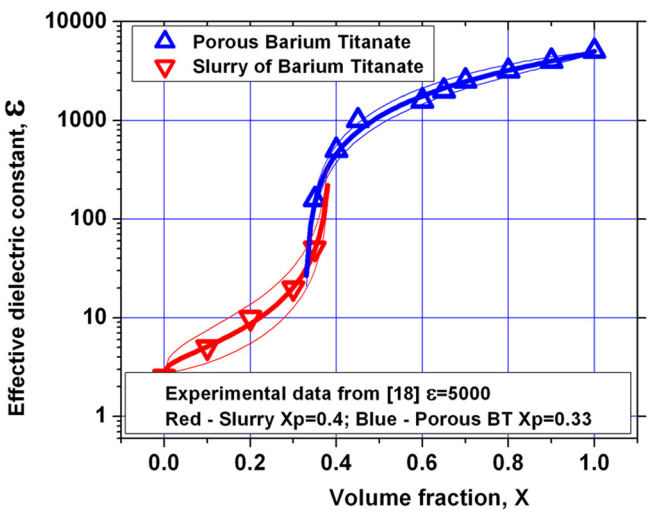

FIG. 2. Introduction of percolation in brick wall models allows extending this approach on real two phase system.[17] Down triangles and red lines are for slurries; up triangles and blue lines are for porous ceramics; thin lines are for models 1 and 2 and thick lines for their averaging.

this fitting. Percolation thresholds Xp were calculated using α and equation $X_1 = \alpha a^3$. Equations (1) and (2) with these values of calculated parameters were then used to demonstrate areas of possible deviations in the model (thinner lines in Fig. 2).

Fig. 2 shows that application of the modified brick wall model results in a good fitting of experimental data for dispersed powder (red curves) as well as for porous ceramic (blue curves). Model 1* and Model 2* surrounds experimental data points over the entire range of X_1 (thin lines) while the averaging equation (3) follows exactly the experimental points. Calculated values of percolation threshold, $X_{1P} = 0.4$ for slurries and $X_{1P} = 0.33$ or $X_{2P} = 0.67$ for porous ceramics, are reasonably within the range of percolation for spherical particles. These results indicate that the modified brick wall model (Eqs. (1)–(3)) can be suggested as a universal model for dielectric two phase systems at least within a reasonable range of percolation thresholds. This model has a clear physical background, and insures good fitting to experimental data obtained from actual two phase systems.

EXTENSION ON MIXED CONDUCTING SYSTEMS

In the above discussion, both phases in a two phase systems were considered as pure dielectrics, i.e., both phases are electrically insulating (no leakage current) or the data were collected at frequencies high enough to neglect the impact of material's conductivity (usually in the range 100 kHz to 10 MHz for slurries[19–21]). Under these assumptions, the effective permittivity ε_{eff} has no frequency dependence. It is the only parameter which can be determined using Eqs. (1)–(3) from experimental measurements of two phase system. Several samples with different ratios between the phase volumes should be measured to obtain additional information on individual components of two phase systems (such as percolation threshold X_P and the values of permittivity of each phase).

Presence of some leakage in one of the phases leads to frequency dependence of ε_{eff} so that impedance spectroscopy technique can be applied to extract additional parameters from impedance spectra of slurries. The shape of impedance spectra depends on the phase that is leaky or electrically conductive. A transition from brick wall model to equivalent electrical circuit can be accomplished by similar way as for pure dielectric systems explained earlier. Notations used in equivalent circuits are combinations of R and C parameters as well as distributed elements (like constant phase element CPE) which are standard notations for equivalent circuits and corresponding fitting software (like Z-VIEW). Transition from this notation to effective parameters of composite material is achieved by normalizing of all parameters to sample geometry to obtain ρ_{eff} and ε_{eff} Physical models as Eqs. (1)–(3) can be applied to extract parameters of each component from the effective parameters of the two-phase system.

Mixed conductive particles dispersed in a dielectric host material represent a simple case as shown in Fig. 3. Transition from brick wall model to equivalent electrical circuit $C_{2B} - R_1/(C_{2A} + C_1)$ is illustrated in Figs. 3(a) and 3(b) and corresponding impedance spectra is shown in Figs. 3(c) and 3(d). It is obvious that suspended particles behave as pure dielectric at high enough frequencies >10 kHz since resistor R_1 is shorted by parallel capacitors $(C_{2B} + C_1)$, so that Eqs. (1)–(3) can be used. Series connection of C_{2B} and $(C_{2A} + C_1)$ defines ε_{eff} by neglecting the influence of resistor R_1 on the

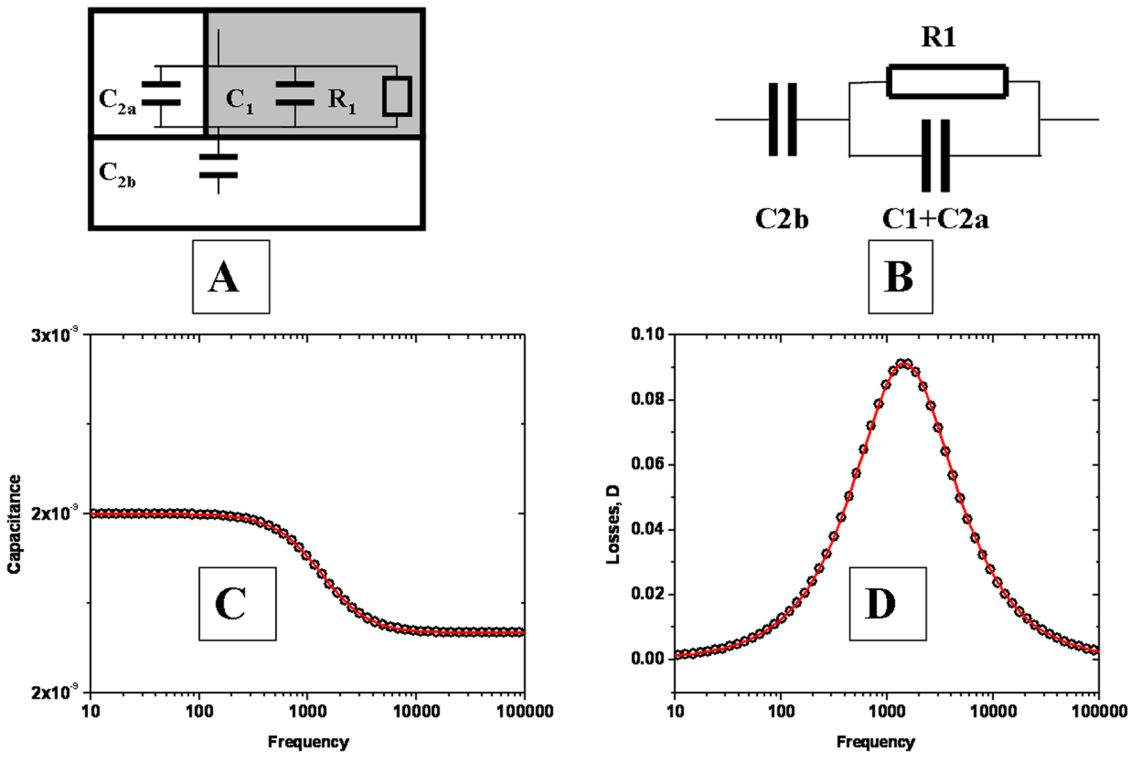

FIG. 3. Impedance spectra of two phase system with conductive suspended and nonconductive host phase (simulation). (a) Example of brick wall model; (b) corresponding equivalent circuit; (c) and (d) capacitance and dielectric losses spectra.

impedance spectra at high frequency. Suspended particles transform from a pure dielectric to a mixed conductor at the Maxwell relaxation frequency. The $R_1/(C_{2A}+C_1)$ element relaxes due to domination of ohmic leakage R_1 so that ε_{eff} is defined only by C_{2B} at low frequencies <100 Hz. The Maxwell relaxation frequency is described as

$$f = 1/(2\pi\rho\varepsilon) = 1/(2\pi R_1{}^*(C_{2A}+C1)). \quad (4)$$

The overall relaxation process is shown by frequency dependences of capacitance and dielectric losses in Fig. 3. Three parameters can be extracted from impedance spectra for each sample: (1) ε_{eff} (H) at high frequency described by Eqs. (1)–(3), (2) transition frequency **f** described by Maxwell equation (4), and (3) ε_{eff} (L) at low frequency described by Eqs. (1)–(3) with indefinitely high value of ε_1, whereas the suspended phase 1 completely shorts the electrical field due to the dominating leakage current. The value of ε_{eff} (L) can be derived from Eqs. (1)–(3) as

Averaging of models(1^*) and (2^*) for indefinitely high dielectric contrast $(\varepsilon_1/\varepsilon_2 \to \infty)$:

$$\frac{\bar{\varepsilon}_{EFF}}{\varepsilon_2} = \frac{(1-(X_1\alpha^2)^{1/3}+X_1)^{0.5}}{1-(X_1\alpha^2)^{1/3}}. \quad (5)$$

Dielectric particles dispersed in mixed conductive host material represent a more complex case of two phase systems (Fig. 4). Transition from brick wall model to equivalent electrical circuit is illustrated in Fig. 4(a) and corresponding impedance spectra is shown in Figs. 4(b)–4(d). In this case, the equivalent circuit consists of two relaxing elements (R_{2B}/C_{2B} and R_{2A}/CPE) so that at least four parameters can be extracted from impedance spectra.[15] First element of the equivalent circuit describes the Maxwell relaxation in host material (red curve marked as Z″-high frequency in Fig. 4(b). This element contains information related with electrical properties of the host material. Equations (4) and (5) describe relationship between parameters of the semicircle corresponding to (R_{2B} and C_{2B}) and properties of the host material ($\boldsymbol{\varepsilon_2}$ and $\boldsymbol{\rho_2}$). The second element describes redistribution of electrical field around suspended particles (blue curve marked as Z″-high frequency in Fig. 4(b)). It was previously reported that permittivity of suspended particles $\boldsymbol{\varepsilon_1}$ can be calculated directly from the low frequency semicircle.[12–15]

The low frequency semicircle appears in impedance spectra if conductivity of the host liquid is high enough to have a complete relaxation of the electrical field in the sample within the frequency range of the impedance spectrometer (0.1 Hz to 1 MHz).[12] In many practical cases, the conductivity of the host material is low so that only high frequency semicircle (or section of it) appears in real impedance spectra, so values of R_{2A} and CPE cannot be achieved from impedance spectra. For this case, the frequency dependences of capacitance and dielectric loss are shown in Figs. 4(c)and 4(d). Experimental data (black circles) and fitting for R_{2b}/C_{2b} relaxation (red curve) in Fig. 4(c) show plateaus at high frequencies, but the levels of these plateaus are different since the experimental data follow Eqs. (1)–(3) while the R_{2b}/C_{2c} fittings follow Eqs. (4) and (5), i.e., information about $\boldsymbol{\varepsilon_1}$ still present in impedance spectra. Difference between values of ε_{eff} measured directly at high

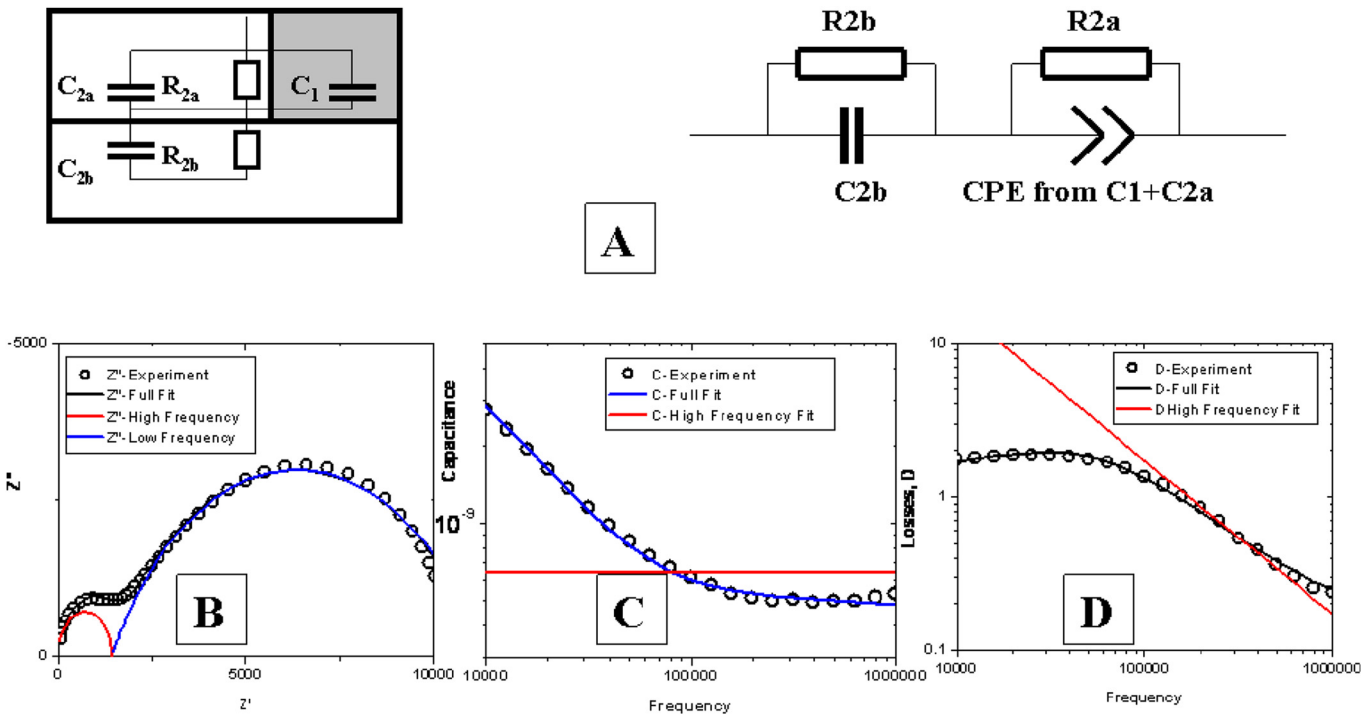

FIG. 4. Impedance spectra of two phase system with nonconductive suspended and conductive host phase (slurry of barium titanate powder dispersed in butoxyethanol). Circles—experimental data, black line—fitting by full equivalent circuit (a); red line—high frequency part of relaxation (R1-C1 element); blue line—low frequency part of relaxation (R2-CPE2 element). (a) Example of brick wall model and corresponding equivalent circuit; (b) experimental impedance spectra (Z′-Z″, full frequency range); (c) and (d) capacitance and dielectric losses data in high frequency range.

frequency (ε_h) and calculated from high frequency semicircle (ε_c) allows calculating values of permittivity for both phases ($\boldsymbol{\varepsilon_1}$ and $\boldsymbol{\varepsilon_2}$) from the high frequency part of impedance spectra without analyzing of low frequency semicircle. This approach can be useful for various two phase systems which do not exhibit low frequency semicircle in the available frequency (0.1Hz to 10 MHz).

Experimental studies of different slurries were conducted to confirm the theoretical approaches described above. Slurries were prepared by dispersing of various dielectric powders in several host liquids. Dielectric powders were BTO, strontium titanate (STO), calcium titanate (CTO), and titanium dioxide (TO). Butoxyethanol (BOE), ethylene glycol (EG), and propylene carbonate (PC) were used as host liquids. Preparation of slurries is described in detail in Ref. 13. Two values of effective permittivity were derived from the high frequency part of impedance spectra: ε_h was measured directly at 0.5 MHz while ε_c was calculated from the high frequency semicircle. While Eqs. (1)–(3) were used for fitting of $\varepsilon_h(X_1)$ dependences, Eq. (5) was applied to fit $\varepsilon_c(X_1)$ dependences for all samples investigated. It was suggested that parameters of slurries (ε_1, ε_2, and X_P) do not depend on solids loading for each type of slurry (i.e., they are not a function of X_1).

The results of this study are summarized in Figs. 5 and 6. Fig. 5 (left) shows the results for slurries prepared by dispersing of different powders in the same solvent (BOE). Red down triangles and blue up triangles represent ε_c (X_1) and ε_h (X_1), respectively. Corresponding curves are obtained by fitting of experimental data with Eq. (5) and Eqs. (1)–(3) for ε_c (X_1) and ε_h (X_1), respectively. These fitting procedures generate parameters of slurry components (ε_1, ε_2, and X_P) shown as inserts for each type of slurry. It is revealed that the applied models result in good fitting with the experimental data and provide reasonable values of slurry parameters. The same experimental data were rearranged in Fig. 5 (right). Upper picture (E) shows ε_c (X_1) dependences for a different powder compositions. It can be seen that ε_c (X_1) is insensitive to the type of powder in the slurry which confirms the suggestion that only the host liquid is responsible for high frequency semicircle and justifies the use of Eq. (5). It allows calculating of permittivity ε_2 of the host liquid and the critical volume fraction of powder at which percolation X_P takes place. Since the permittivity ε_1 of powder is not considered in Eq. (5), it cannot be extracted from ε_c (X_1) dependences. In the contrary, the value of ε_h (X_1) is sensitive to the type of powder as shown in Fig. 5(f) so that Eqs. (1)–(3) should be used in this case to calculate the values of ε_1.

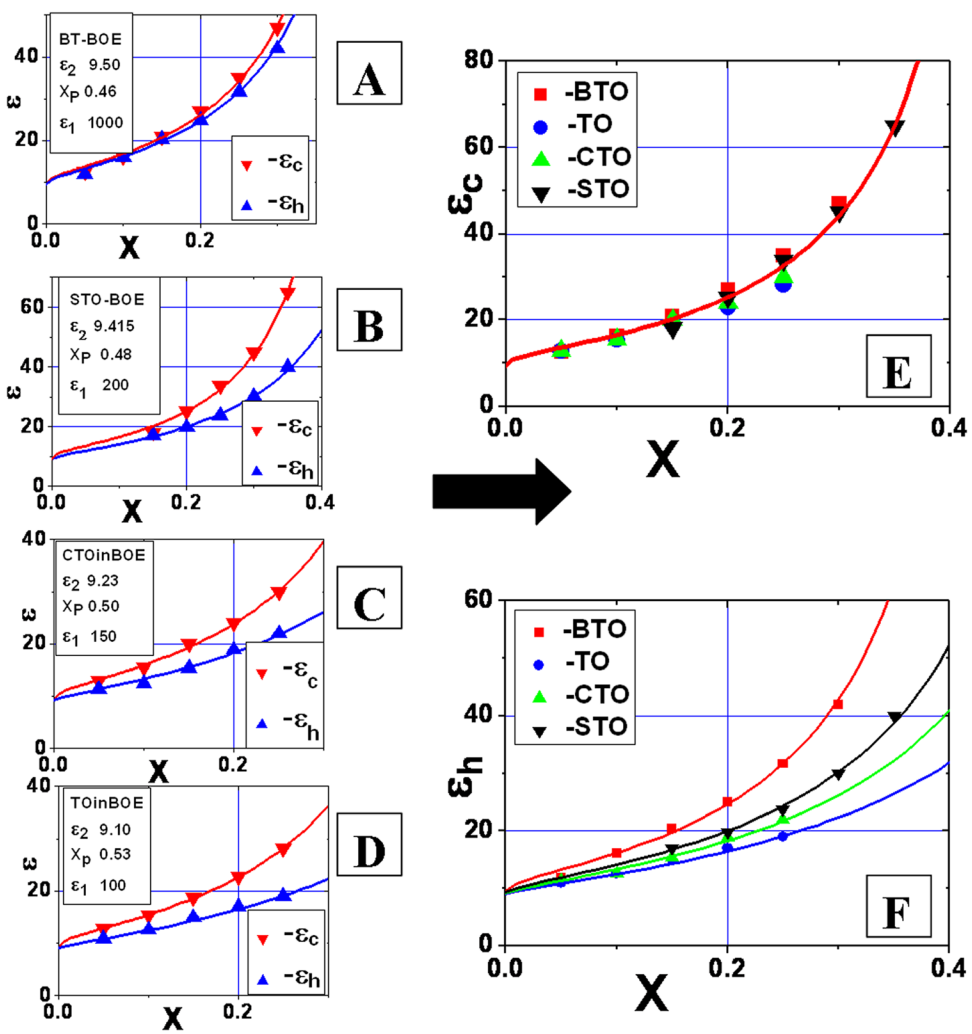

FIG. 5. Dependences of high frequency permittivity ε_h and permittivity calculated from high frequency semicircle ε_c for various powders in BOE. (a) BTO, (b) STO, (c) CTO, (d) TO; (e) ε_c dependence for all powders, (f) ε_h dependence for all powders.

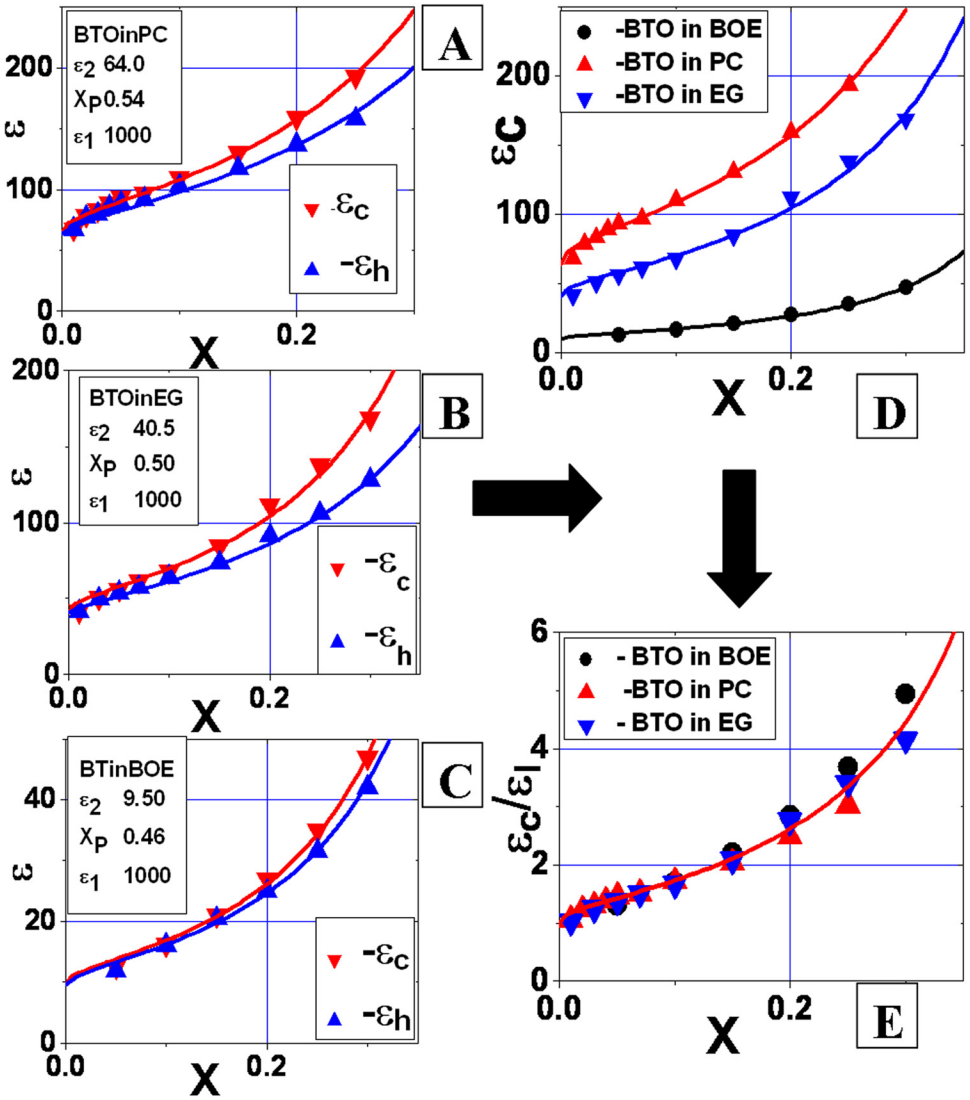

FIG. 6. BT powder dispersed in different liquids. Dependences of high frequency permittivity and permittivity calculated from high frequency semicircle. (a) PC, (b) EG, (c) BOE; (d) ε_c dependence for all liquids, (e) ε_c / ε_1 ratios for all liquids.

Influence of host liquid properties on the impedance spectra is shown in Fig. 6. Left three pictures in Fig. 6 show the results for slurries prepared by dispersing of BTO powder in different solvents. Red down triangles represent ε_c (X_1), blue up triangles represent ε_h (X_1), and corresponding curves were obtained by fitting of experimental data with Eqs. (1)–(3) and (5). Good fitting quality and reasonable values for slurry parameters were obtained. Fig. 6 shows also the same experimental data after rearrangement on right side of the figure. Fig. 6(d) reveals ε_c (X_1) dependences for all three host liquids. It is shown that ε_c (X_1) is shifted proportionally to permittivity of corresponding liquid. Normalized values of effective permittivity $\varepsilon_c/\varepsilon_2$ are shown in Fig. 6(e) indicating that differences between the slurries are compensated and validating the use of Eq. (5) for ε_c (X_1) dependences.

Table I shows permittivity values for various powders (ε_1) and liquids (ε_2) as well as percolation threshold (X_{1p}). These values were calculated from high frequency part of the impedance spectra using Eqs. (1)–(3) and (5). For all slurries investigated, threshold values are close to 0.5 that are reasonable for well dispersed particles of nearly spherical shape. The calculated values of permittivity of liquids are reproducible and in good agreement with the literature data.

Fitting accuracy of permittivity for powders depends on the value of dielectric contrast. For a low contrast case (TO-BOE), the difference between ε_c and ε_h is large enough so that ε_1 is well defined while for high contrast (BTO-BOE), the difference between ε_c and ε_h is small so that the value of ε_1 can be only estimated. However, the relationships obtained from the high frequency part of impedance spectra are opposite to that for the low frequency part as shown in Table II. Values of permittivity ε_1 measured for bulk sintered samples and ε_1 calculated from the low and high frequency

TABLE I. The values of permittivity of liquids and powders and percolation parameters of corresponding slurries calculated from high frequency parts of impedance spectra.

Liquid	Powder	ε_1	ε_2	X_P
PC	BTO	~1000	64.0	0.54
EG	BTO	~1000	40.5	0.50
BOE	BTO	~1000	9.5	0.46
BOE	STO	200	9.4	0.48
BOE	CTO	150	9.2	0.50
BOE	TO	100	9.1	0.53

TABLE II. Comparison of permittivity values of bulk materials with the values calculated from low frequency[13] and high frequency parts of impedance spectra.

Material	TO	CTO	STO	BTO
Bulk	86–173	198	300–310	1200–3000
Low F sc	142 ± 5	210 ± 8	300 ± 10	1400 ± 50
High F sc	100	150	200	~1000

sections of slurry impedance spectra are compared. While the low frequency part of the spectra provides a better accuracy in determining the permittivity ε_1 of powders in slurries of low permittivity contrast, the high frequency part provides a better accuracy for slurries of high permittivity contrast.

CONCLUSIONS

Extension of brick wall model on two phase systems with percolation provides a solid basis for theoretical characterization of pure dielectric systems. Corresponding equations can also be applied to the systems with mixed conductivity. The values of permittivity of both phases as well as percolation threshold can be calculated from low frequency as well as high frequency sections of the impedance spectra for a given two phase system. Experimental investigations of various slurries confirm the theoretical predictions. Theoretical equations, developed in this study, provide a good fitting to experimental data. Calculated parameters of slurry components are in good agreement with previous measurements of slurries and the literature data for corresponding bulk materials.

[1]D. S. McLachlan, M. Blaszkiewscz, and R. E. Newnham, "Electrical resistivity of composites," J. Am. Ceram. Soc. **73**(8), 2167–2203 (1990).
[2]K. Lal and R. Parshad, "The permittivity of heterogeneous mixtures," J. Phys. D: Appl. Phys. **6**, 1363 (1973).
[3]L. Jylha and A. Sihvola, "Differential equation for the effective permittivity of random mixture of spheres," in EMTS 2007–International URSI Commission B–Electromagnetic Theory Symposium, Ottawa, Canada, 26–28 July 2007.
[4]D. S. McLachlan, J. H. Hwang, and T. O. Mason, "Evaluating dielectric impedance spectra using effective media theories," J. Electroceram. **5**(1), 37–51 (2000).
[5]N. Bonanos, B. C. H. Steele, and E. P. Butler, "Applications of impedance spectroscopy," in *Impedance Spectroscopy*, 2nd ed., edited by E. Barsoukov and J. Ross Macdonald (John Wiley & Sons, Hoboken, New Jersey, 2005), pp. 205–227.
[6]N. J. Kidner, Z. J. Homerighaus, B. J. Ingram, T. O. Mason, and E. J. Garboczi, "Impedance/dielectric spectroscopy of electroceramics–Part 1: Evaluation of composite models for polycrystalline ceramics," J. Electroceram. **14**, 283–291 (2005).
[7]N. J. Kidner, Z. J. Homerighaus, B. J. Ingram, T. O. Mason, and E. J. Garboczi, "Impedance/dielectric spectroscopy of electroceramics–Part 1: Grain shape effects and local properties of polycrystalline ceramics," J. Electroceram. **14**, 293–301 (2005).
[8]T. Ohno, D. Suzuki, K. Ishikawa, M. Horiuchi, T. Matsuda, and H. Suzuki, "Size effect for Ba(ZrxTi1x)O3 (x50.05) nano-particles," Ferroelectrics **337**, 25–32 (2006).
[9]K. A. Goswami, "Dielectric Properties of Unsintered Barium Titanate," J. Appl. Phys. **40**(2), 619–624 (1969).
[10]A. Biswas, I. S. Bayer, P. C. Karulkar, A. Tripathi, D. K. Avasthi, M. G. NortonSzczech, and J. B. Szczech, "Nanostructured barium titanate composites for embedded radio frequency applications," Appl. Phys. Lett. **91**(21), 212902 (2007).
[11]Z. Dang, Y. Zheng, and H. Xu, "Effect of the ceramic particle size on the microstructure and dielectric properties of barium titanate/polystyrene composites," J. Appl. Polym. Sci. **110**(6), 3473–3479 (2008).
[12]V. Petrovsky, A. Manohar, and F. Dogan, "Dielectric constant of particles determined by impedance spectroscopy," J. Appl. Phys. **100**(1), 014102 (2006).
[13]V. Petrovsky, T. Petrovsky, S. Kamlapurkar, and F. Dogan, "Characterization of dielectric particles by impedance spectroscopy (part I)," J. Am. Ceram. Soc. **91**(6), 1814 (2008).
[14]V. Petrovsky, T. Petrovsky, S. Kamlapurkar, and F. Dogan, "Physical modeling and electrodynamic characterization of dielectric slurries by impedance spectroscopy (part 11)," J. Am. Ceram. Soc. **91**(6), 1817–1819 (2008).
[15]P. Jasinski, V. Petrovsky, and F. Dogan, "Impedance spectroscopy of $BaTiO_3$ cubes suspended in lossy liquids as a physical model of two-phase system," J. Appl. Phys. **108**, 074111 (2010).
[16]W. T. Doyle, "Particle clustering and dielectric enhancement in percolating metal-insulator composites," J. Appl. Phys. **78**(10), 6165–6169 (1995).
[17]V. Petrovsky, P. Jasinski, and F. Dogan, "Effective dielectric constant of two phase dielectric systems," J. Electroceram. **28**,185–190 (2012).
[18]W. Huebner, F. C. Jang, and H. U. Anderson, "Dielectric and electrical properties of $BaTiO_3$ composites," in *Multiphase and Composite Ceramics*, edited by C. G. Pantano, R. E. Tressler, G. L. Messing, and R. E. Newnham (Plenum Publishing Corporation, 1986), pp. 433–442.
[19]S. Wada, H. Yasuno, T. Hoshina, S.-M. Nam, H. Kakemoto, and T. Tsurumi, "Preparation of NM-sized barium titanate fine particles and their powder dielectric properties," Jpn. J. Appl. Phys., Part 1 **42**(9B) 6188–6195 (2003).
[20]S. Wada, T. Hoshino, H. Yasuno, M. Ohishi, H. Kakemoto, T. Tsurumi, and M. Yashima, "Dielectric properties of NM-sized barium titanate fine particles and their size dependence," Ceram. Eng. Sci. Proceed. **26**(5) 89–100 (2005).
[21]T. Tsurumi, T. Sekine, H. Kakemoto, T. Hoshina, S.-M.Nam, H. Yasuno, and S. Wada, "Evaluation of dielectric permittivity of barium titanate fine powders," 2004 MRS Fall Meeting. Materials, integration and packaging issues for high-frequency devices II, 833, G7.5. Mater. Res. Soc. Sym. Proc. **833**, 243–247 (2005).